NACA

RESEARCH MEMORANDUM

FLIGHT INVESTIGATION TO DETERMINE LIFT AND DRAG CHARACTERISTICS OF A CANARD RAM-JET MISSILE CONFIGURATION IN THE MACH NUMBER RANGE OF 0.8 TO 2.0

By Abraham A. Gammal and Thomas L. Kennedy

Langley Aeronautical Laboratory
Langley Field, Va.

NATIONAL ADVISORY COMMITTEE
FOR AERONAUTICS

WASHINGTON
June 17, 1954

NATIONAL ADVISORY COMMITTEE FOR AERONAUTICS

RESEARCH MEMORANDUM

FLIGHT INVESTIGATION TO DETERMINE LIFT AND DRAG CHARACTERISTICS OF A CANARD RAM-JET MISSILE CONFIGURATION IN THE MACH NUMBER RANGE OF 0.8 TO 2.0

By Abraham A. Gammal and Thomas L. Kennedy

SUMMARY

A flight investigation has been conducted on a canard ram-jet missile configuration to determine its lift and drag characteristics at low values of lift. The configuration consists of two ram-jet engines mounted on a composite wing having leading-edge sweepback of 0° inboard of the engines and 60° outboard of the engines; the canard is of the delta type with a 60° leading-edge sweepback angle. Two rocket-boosted models, differing only in the size and deflection of the canard, were employed in the investigation.

The lift and drag data were obtained in the Mach number range of 0.8 to 2.0 with the Reynolds number varying from 3×10^6 to 14×10^6, based on wing root chord.

It was found that in the supersonic speed range of the tests the effectiveness of the canards in producing model lift is nearly directly proportional to their exposed areas.

INTRODUCTION

In recent years, there has been an increasing interest in canard missiles capable of cruising at supersonic speeds. One of the problems associated with such configurations is that of properly assessing the effect that a canard has on the aerodynamics of the missile. Experimental aerodynamic characteristics for canard configurations having conventional wing shapes are presented in references 1, 2, 3, and 4 and a method for predicting lift and center of pressure is presented in reference 5. Because of the unconventional wing configuration which occurs

when wing-mounted ram jets are used, with a portion of the wing extending outboard of the ram jets, the data of above references cannot be readily compared with this configuration. Therefore, the Langley Pilotless Aircraft Research Division has conducted a flight investigation on a canard wing-mounted ram-jet engine configuration suitable for application as a cruising missile.

Flight tests were made at the Pilotless Aircraft Research Station at Wallops Island, Va., to determine the lift and drag characteristics of the configuration under trim conditions and the effect of varying the canard size on these characteristics. Two models, differing essentially only in canard size and deflection, were employed in the investigation and the desired data obtained in the Mach number range of 0.8 to 2.0. The flight technique was such that some information on longitudinal stability characteristics was obtained in each flight at approximately the maximum Mach number of the individual flight.

SYMBOLS

b	exponential damping constant in e^{-bt}, per sec
c	wing root chord, ft
M	Mach number
P	period, sec
p_B	base pressure
p_o	free-stream static pressure
q	dynamic pressure, $\frac{1}{2}\rho V^2$
R	Reynolds number based on wing root chord
S_C	exposed canard area, sq ft
S_W	wing reference area, sq ft
V	velocity
α	angle of attack, deg
δ	canard deflection, deg

C_D drag coefficient based on wing reference area

C_L lift coefficient based on wing reference area

C_m pitching-moment coefficient based on wing reference area and root chord

C_p nacelle annular base pressure coefficient, $\frac{p_B - p_o}{q}$

$C_{m_\alpha} = \frac{\partial C_m}{\partial \alpha}$

Subscripts:

A model A

B model B

trim trim condition

MODEL DESCRIPTION

Configurational features of the two models tested are indicated in figure 1. The prime difference between the two models is the canard size; the model with the smaller canard is designated model A and that with the larger canard, model B. Photographic top and side views of model B are presented as figure 2.

Integral with the wing are twin ducted nacelles, the external lines of which simulate a twin-engine ram-jet installation; internally, the ducts have a constant diameter of 2.70 inches and thus produce an annular surface at the base of the nacelles. The thickness ratio of the inboard section of the wing is 0.044 and that of the outboard section at the nacelle juncture is 0.030. The wing reference area, taken to be the area bounded by the curve consisting of the leading and trailing edges of the inboard and outboard wing sections and their extensions to the point of intersection, is 1.517 square feet.

The canard of both models is of the delta type and has a 60° leading-edge sweepback angle; details are given in figure 3. The ratio of exposed canard area to wing reference area is 0.0211 and 0.0458 for models A and B, respectively. Considering the part of the body intercepted by the canard leading and trailing edges as included in the total canard area, the ratio of the total canard area to the wing reference area is 0.0533 and 0.0817 for models A and B, respectively.

Inasmuch as the usual vane-type angle-of-attack indicator available was large relative to the size of the canards employed and therefore very likely would unduly influence the flow field about the model, the angle of attack was obtained by measuring the pressure differences between the upper and lower surfaces of a cone. The nose of the model, near its tip, was accordingly made a 30° cone.

Weight and pitch moment of inertia were 73.9 pounds and 8.32 slug-feet^2 for model A and 66.9 pounds and 8.05 slug-feet^2 for model B.

INSTRUMENTATION

Both models contained a four-channel NACA telemetering system capable of continuously transmitting normal and longitudinal acceleration, nose-cone differential pressure, and nacelle annular base pressure; the latter was obtained as a manifold pressure at the base of one of the nacelles.

Ground equipment complementary to the flight instrumentation included a CW Doppler radar unit and a radar tracking unit for determination of model speed and trajectory. A radiosonde was used to obtain atmospheric data.

APPARATUS AND TECHNIQUE

The models were boosted to their peak flight Mach numbers by a single-stage booster consisting of two solid-fuel rockets, each capable of delivering an average thrust of about 6,000 pounds for 3.0 seconds. There was no rocket motor contained in the models. A photograph of model B and the booster in the launching position is presented as figure 4.

During the boost phase of the flight, the canard, which was spring loaded, was held in the undeflected position by a pin-locking mechanism, the pin being tied to the model adapter by means of a wire. As the booster separated from the model, it pulled on the locking pin and then broke the wire connection between model and booster. Release of the locking mechanism allowed the canard to flip up to a predetermined deflection; the deflection was 4.92° for model A and 6.06° for model B. The spring held the canard up against a fixed stop at the desired deflection for the remainder of the flight.

The impulse given to the canard caused the model to go through an initial oscillatory phase in pitch followed by essentially a trimmed-out flight condition. Data were obtained during the coasting portion of

the model flight, with the short oscillatory phase providing the data from which the model stability characteristics were obtained.

DATA REDUCTION AND ANALYSIS

For presentation in a more informative and usable form, nacelle internal and annular base drag coefficients were subtracted from the total drag coefficient obtained for the models as tested. Nacelle internal skin-friction coefficient based on the duct wetted area was taken to be 0.0017 (based on data of ref. 6) for the entire Mach number range of the tests. This gave a corresponding internal-drag coefficient of 0.0029 based on the wing reference area of this configuration.

No allowance could be made for the effect of the nacelle internal lift on the model lift, angle of attack, and stability characteristics inasmuch as these correspond to given canard deflections and are consequently interdependent. It may be pointed out, however, that the contribution of the internal lift to the total lift is small, being 2 to 3 percent of the total lift, and that it acts close to the model center of gravity.

The model angle of attack was obtained from the cone differential pressure by using the M.I.T. cone tables (refs. 7 and 8). Angle-of-attack data were obtainable only in the essentially trimmed out portion of the flight for, as expected, in the initial oscillatory portion of the flight the volume in the pressure lines and cell combined with the high rate-of-pressure change to give substantial pressure lag. The angle of attack could not be determined much below $M = 1.30$ because of inapplicability of the cone tables in that range.

Accuracy

On the basis of statistical data compiled by the Langley Instrument Research Division, it is believed that model instrumentation is accurate to within ±1 percent of the full-scale range for pressure measuring instruments and ±1½ percent for the accelerometer-type instruments. The Mach number obtained by Doppler radar is believed to be accurate to ±1 percent.

Based on these assumptions, the following probable quantity errors are listed for a Mach number of 1.8; for a Mach number of 1.3 the probable error would be twice that of the quantities listed:

$C_{D_{trim}}$ . . . . . ±0.007
α_{trim}, deg . . . . . ±0.1
C_p . . . . . ±0.01
$C_{L_{trim}}$ . . . . . ±0.004

RESULTS AND DISCUSSION

Variation of Reynolds number based on wing root chord with flight Mach number for models A and B is shown in figure 5.

Trim Lift Characteristics

Trim lift coefficients for both models are presented in figure 6. Due to lack of angle-of-attack data below a Mach number of 1.3, the trim angle of attack was assumed to be 1.8° for model B and 0.8° for model A. Since these values of angle of attack are small, it is felt that the data below a Mach number of 1.3 represent essentially the trim lift characteristics of the configuration. The difference in the trim lift of the two models is attributable largely to the 117 percent greater exposed canard area of model B, and somewhat to a 23 percent greater canard deflection angle.

The effectiveness of the two canards in producing model lift is indicated in figure 7; the assumption was made that $C_{L_{trim}}$ at $\delta = 0°$ was negligible for the actual models. Figure 8 shows that the trim lift produced by the canards is nearly directly proportional to their exposed areas in the supersonic range of the tests. Use of total, instead of exposed, canard areas would have yielded values for $\frac{S_{C_A}}{S_{C_B}}\left(\frac{\Delta C_{L_{trim}}}{\Delta\delta}\right)_B \Big/ \left(\frac{\Delta C_{L_{trim}}}{\Delta\delta}\right)_A$ greater than 1.42. It should be noted that the ratio of model B canard area to that of model A is 2.17 for exposed area and 1.53 for total area.

Trim angle-of-attack variation with Mach number is presented in figure 9 only for the flight Mach number range from 1.30 to 1.80 for model A and from 1.30 to 1.85 for model B. The reasons for the restricted ranges were indicated under "Data Reduction and Analysis."

The approximate trim lift-curve slope of both models is shown in figure 10. Data of reference 4 indicate that the lift produced by the canard is a negligible amount compared to the total lift of the configuration. Considering the relatively small canards and angle-of-attack range

used in the present tests $C_{L_{trim}}/\alpha_{trim}$ is a good approximation to the lift-curve slope.

Drag

Nacelle annular base manifold-pressure data are presented in figure 11 in the form of pressure coefficient. There is little difference between the pressure coefficients for the two models, which is to be expected in view of the fact that the angle of attack is small for both models and that the canards, the only major difference between the models, are well ahead of the nacelles.

Measured trim drag coefficients minus nacelle internal and nacelle base drag coefficients for models A and B are presented in figure 12. The portions of the curves below $M = 1.30$ are shown dotted because of the lack in that region of angle-of-attack data needed for determining $C_{D_{trim}}$ from the longitudinal- and normal-accelerometer readings; the angle of attack was taken as 0.8° for model A and 1.8° for model B below $M = 1.30$.

Stability

Stability characteristics of the models are presented in the following table; the method of computation is that presented in reference 9. Data are available at only one Mach number for each model because of flight-testing-technique limitation.

Model	M	P	b	C_{m_α}
A	1.85	0.165	2.82	-0.0286
B	2.02	.168	2.57	-.0232

CONCLUDING REMARK

Results of the flight test of two models having a canard wing-mounted ram-jet missile configuration and differing only in the size and deflection of the canard showed that the effectiveness of the canards in producing model lift in the supersonic range of the tests is nearly directly proportional to their exposed areas.

Langley Aeronautical Laboratory,
National Advisory Committee for Aeronautics,
Langley Field, Va., April 15, 1954.

REFERENCES

1. Hamilton, Clyde V., Driver, Cornelius, and Sevier, John R., Jr.: Wind-Tunnel Investigation of a Ram-Jet Missile Model Having a Wing and Canard Surfaces of Delta Plan Form With 70° Swept Leading Edges. Force and Moment Characteristics of Various Combinations of Components at a Mach Number of 1.6. NACA RM L53A14, 1953.

2. Spearman, M. Leroy: Aerodynamic Characteristics in Pitch of a Series of Cruciform-Wing Missiles With Canard Controls at a Mach Number of 2.01. NACA RM L53I14, 1953.

3. Spearman, M. Leroy, and Robinson, Ross B.: Aerodynamic Characteristics of a Cruciform-Wing Missile With Canard Control Surfaces and of Some Very Small Span Wing-Body Missiles at a Mach Number of 1.41. NACA RM L54B11, 1954.

4. Spearman, M. Leroy, and Robinson, Ross B.: Wind-Tunnel Investigation of a Ram-Jet Canard Missile Model Having a Wing and Canard Surfaces of Delta Plan Form With 70° Swept Leading Edges. Longitudinal and Lateral Stability and Control Characteristics at a Mach Number of 1.60. NACA RM L52E15, 1952.

5. Nielsen, Jack N., Kaattari, George E., and Anastasio, Robert F.: A Method for Calculating the Lift and Center of Pressure of Wing-Body-Tail Combinations at Subsonic, Transonic, and Supersonic Speeds. NACA RM A53G08, 1953.

6. Judd, Joseph H.: Flight Investigation of Engine Nacelles and Wing Vertical Position on the Drag of a Delta-Wing Airplane Configuration From Mach Number of 0.8 to 2.0. NACA RM L53L21, 1954.

7. Staff of the Computing Section, Center of Analysis (Under Direction of Zdeněk Kopal): Tables of Supersonic Flow Around Cones. Tech. Rep. No. 1, M.I.T., 1947.

8. Staff of the Computing Section, Center of Analysis (Under Direction of Zdeněk Kopal): Tables of Supersonic Flow Around Yawing Cones. Tech. Rep. No. 3, M.I.T., 1947.

9. Niewald, Roy J., and Moul, Martin T.: The Longitudinal Stability, Control Effectiveness, and Control Hinge-Moment Characteristics Obtained From a Flight Investigation of a Canard Missile Configuration at Transonic and Supersonic Speeds. NACA RM L50I27, 1950.

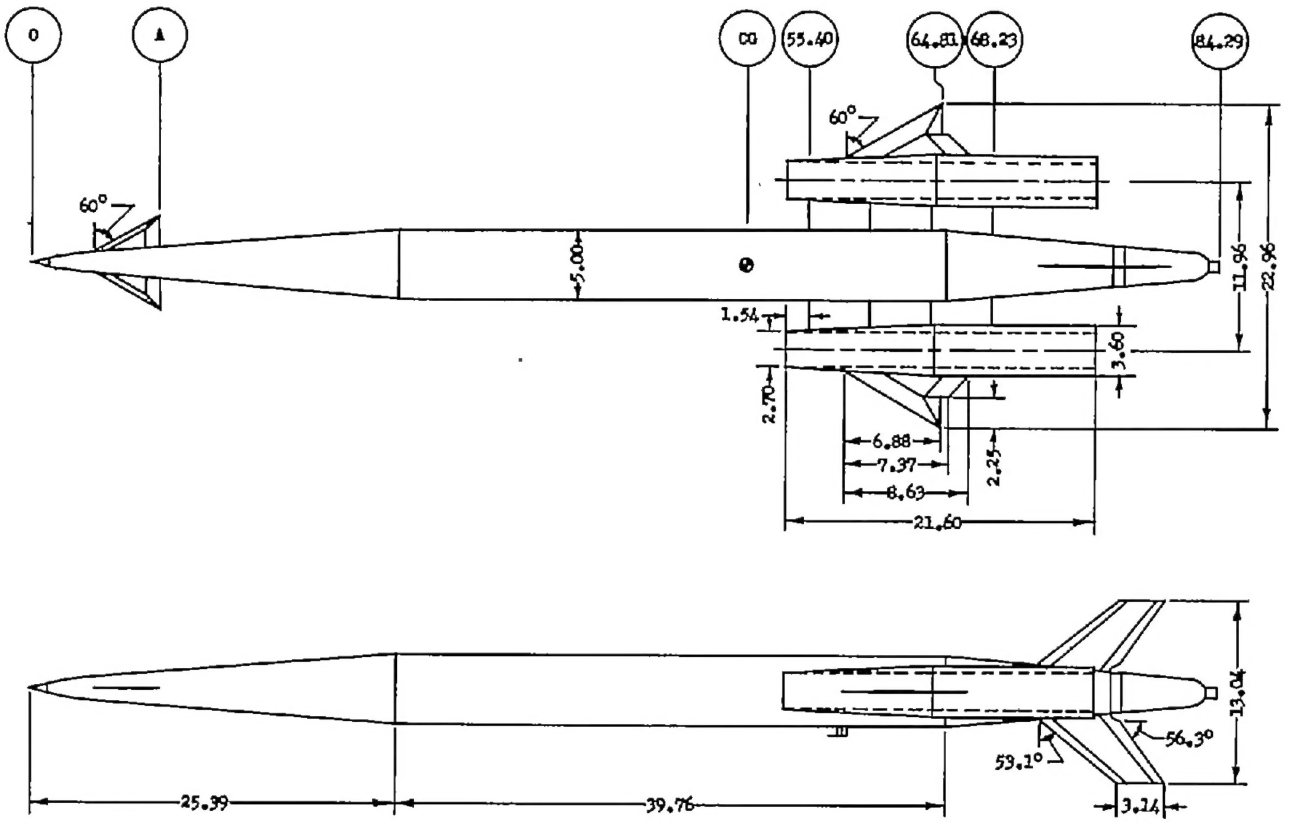

	Model A	Model B
Station A	8.68	9.23
Station CG	50.68	50.52
Exposed canard area, sq ft	.0319	.0694
Total canard area, sq ft	.0808	.1238
Wing reference area, sq ft	1.517	1.517
Canard deflection, deg	4.92	6.06

Figure 1.- Top and side views of model configuration. (All dimensions are in inches.)

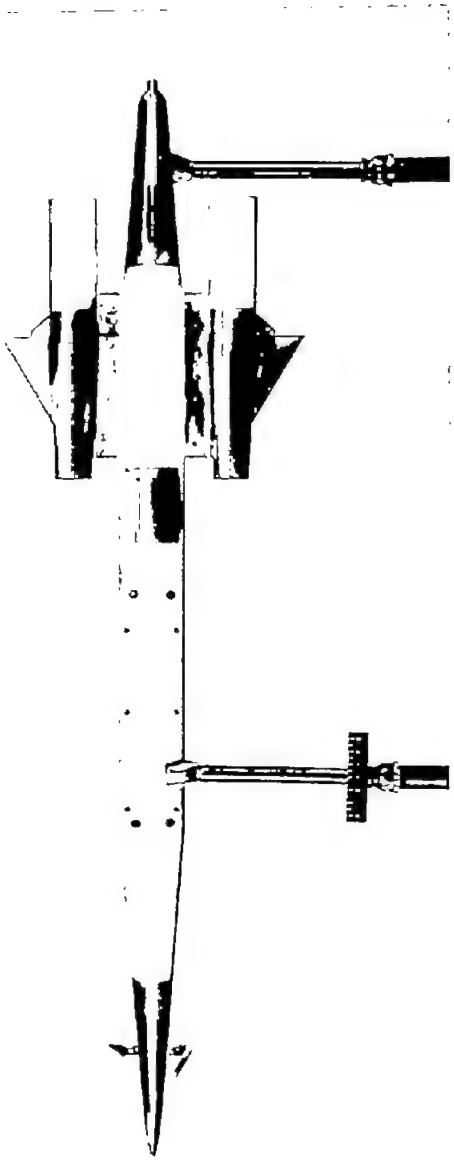

L-78907.1

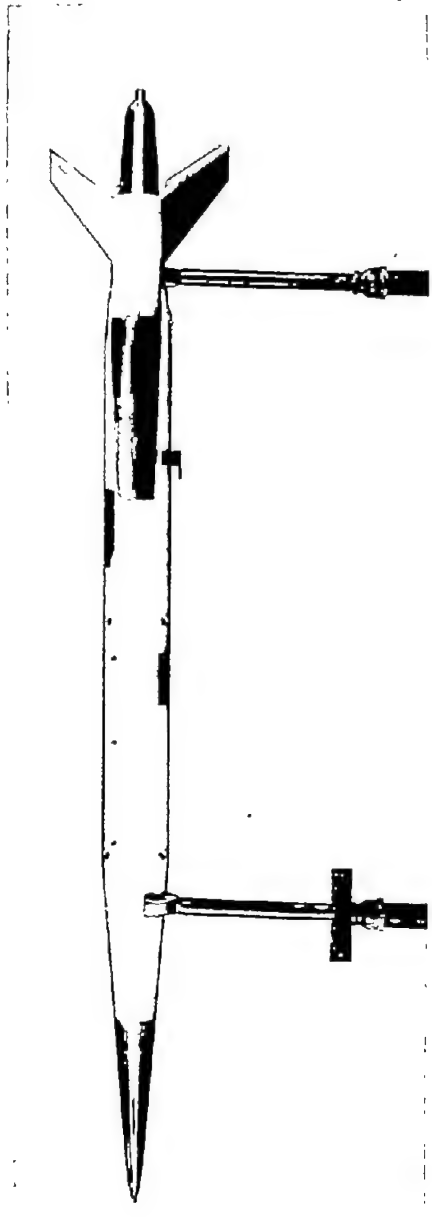

L-78908.1

Figure 2.- Top and side views of model B.

Model B canard

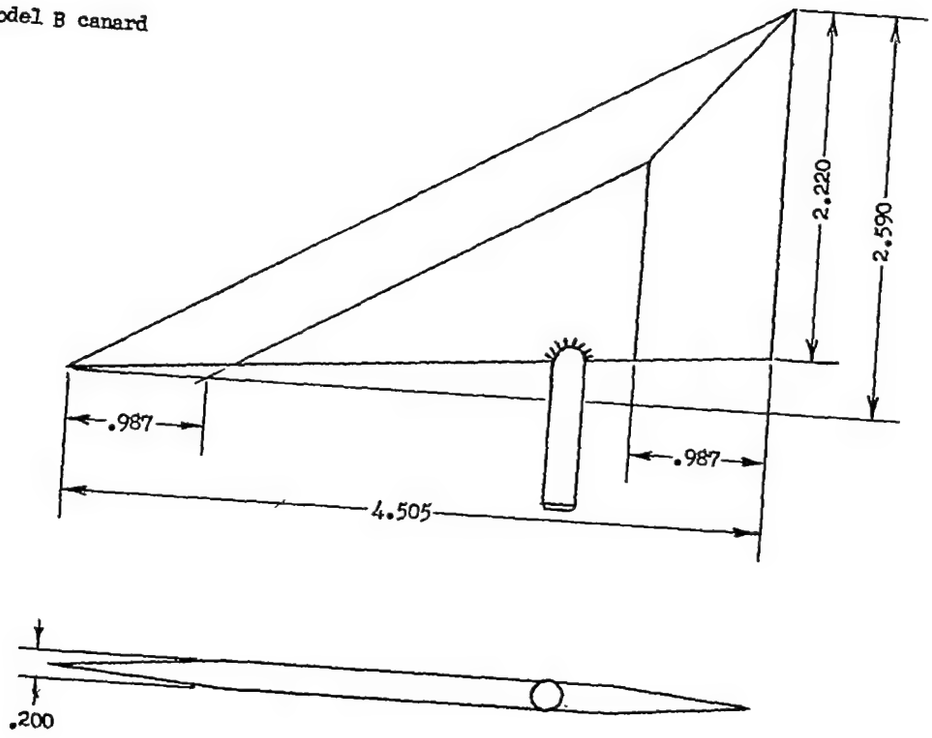

Model A canard

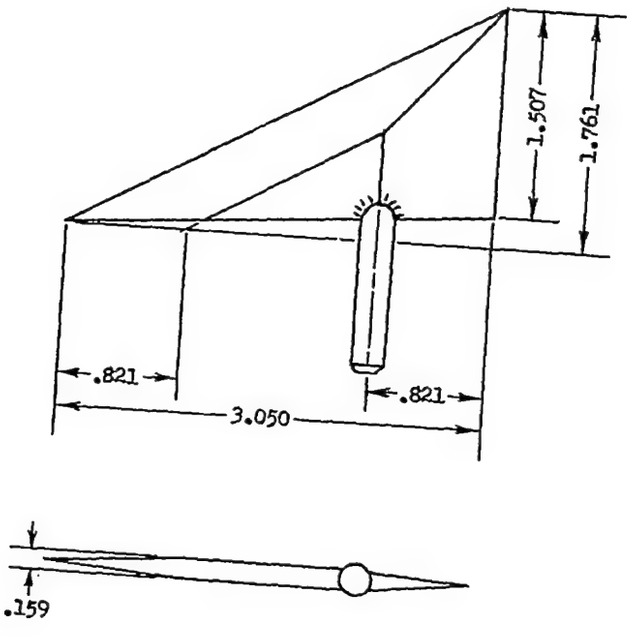

Figure 3.- Canard details. (All dimensions are in inches.)

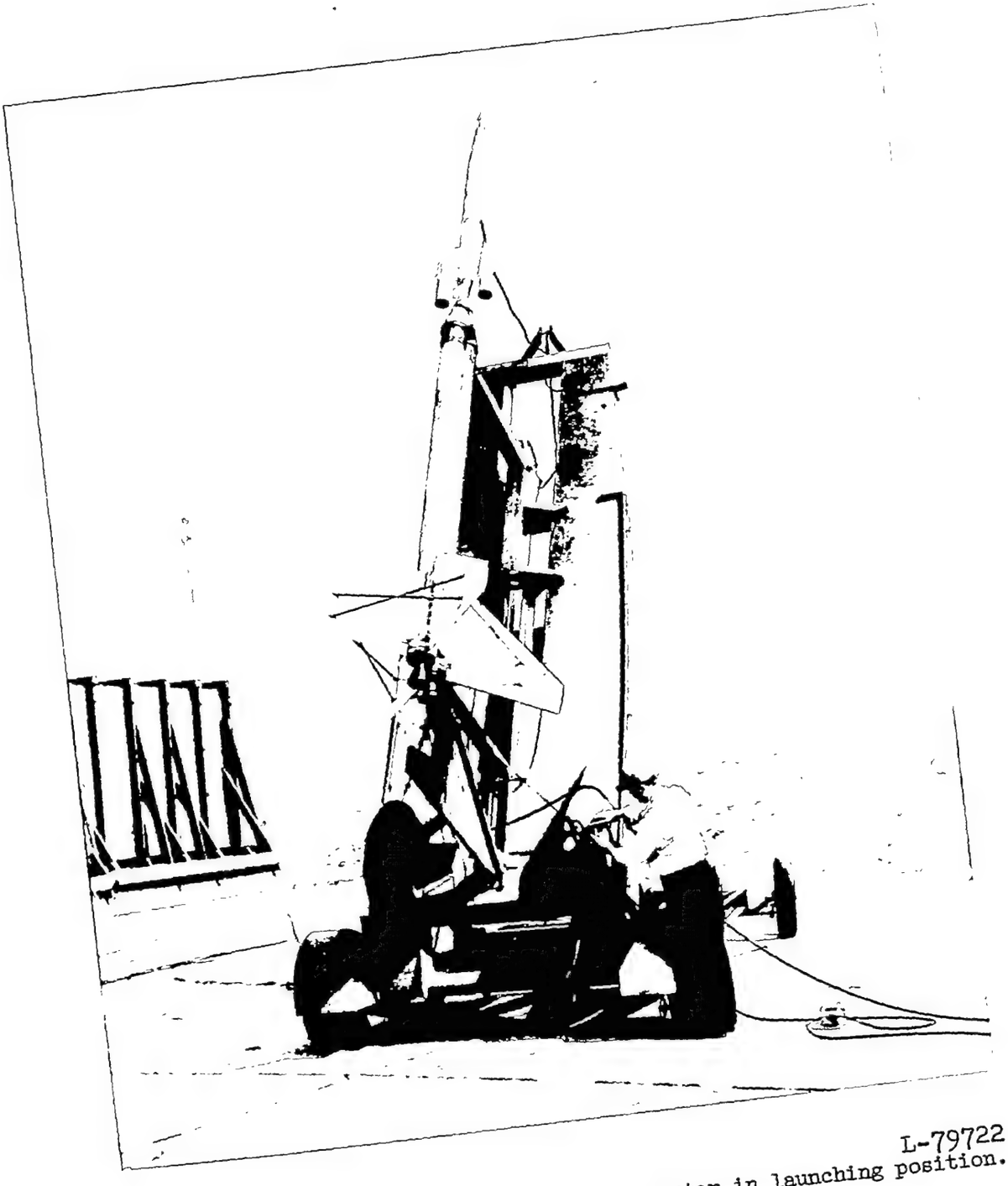

L-79722

Figure 4.- Photograph of model B and booster in launching position.

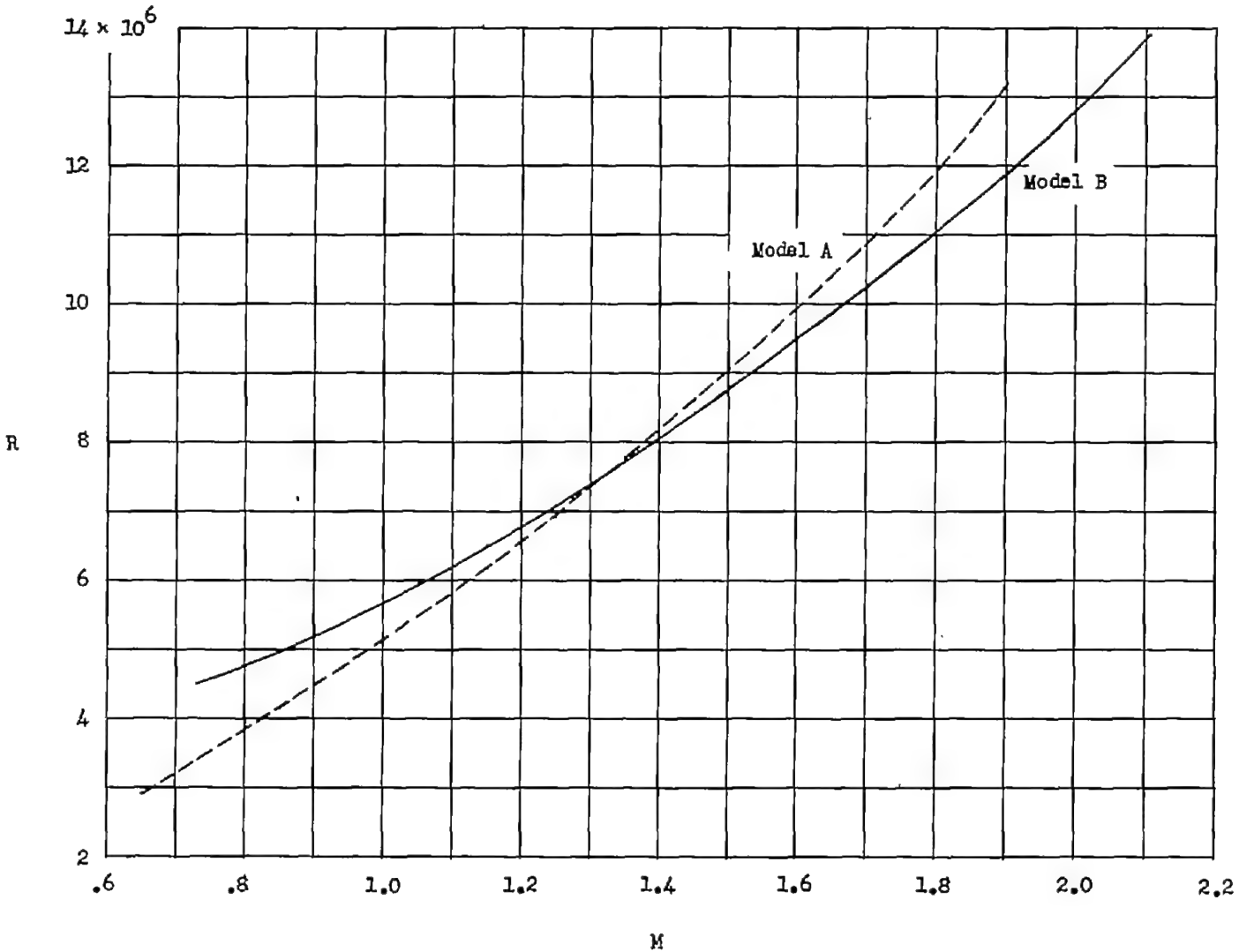

Figure 5.- Reynolds number variation with Mach number. (Reynolds number based on wing root chord.)

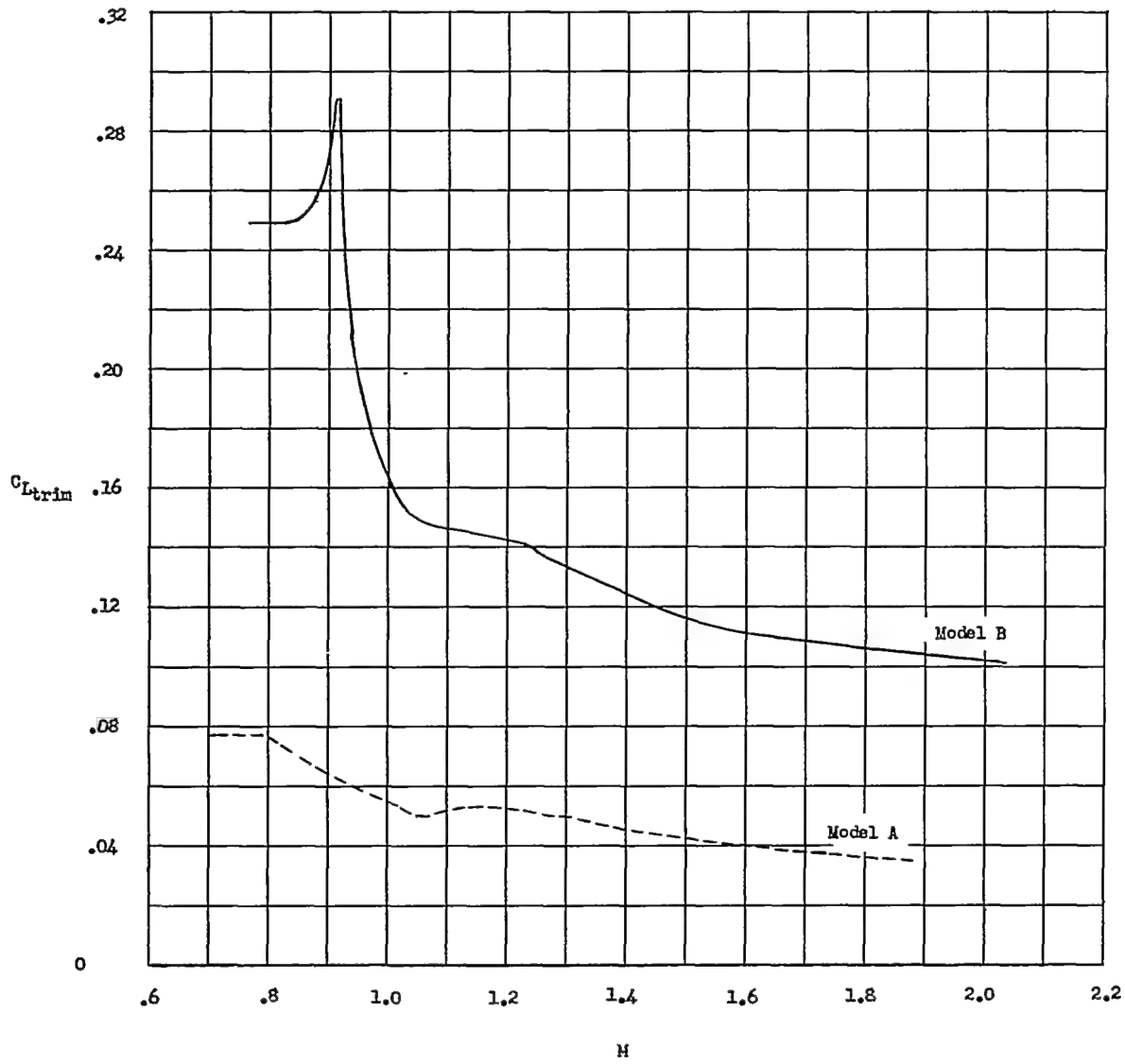

Figure 6.- Trim-lift-coefficient variation with Mach number.

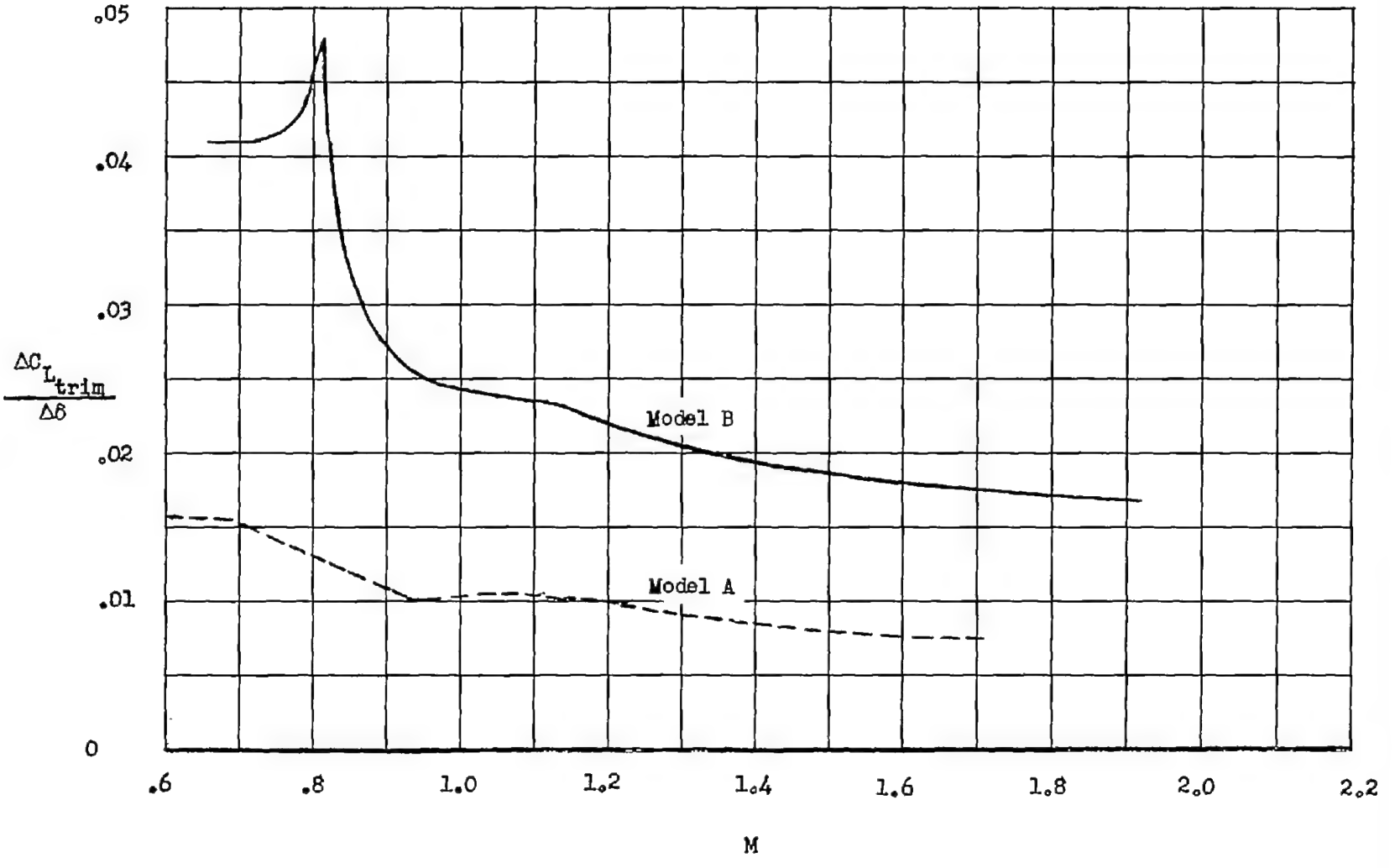

Figure 7.- Canard effectiveness in producing model lift.

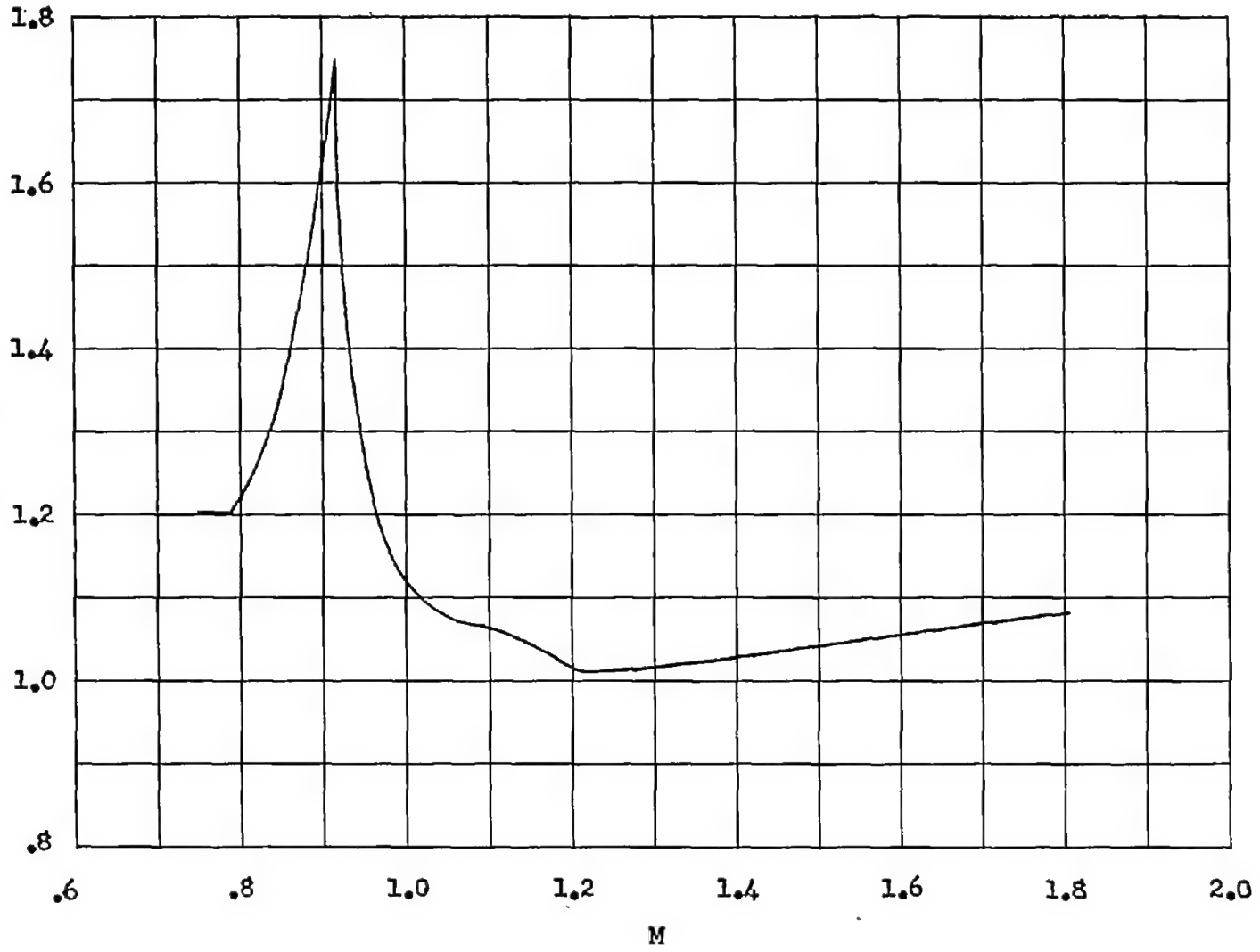

Figure 8.- Trim lift characteristics of canards of models A and B in producing model lift.

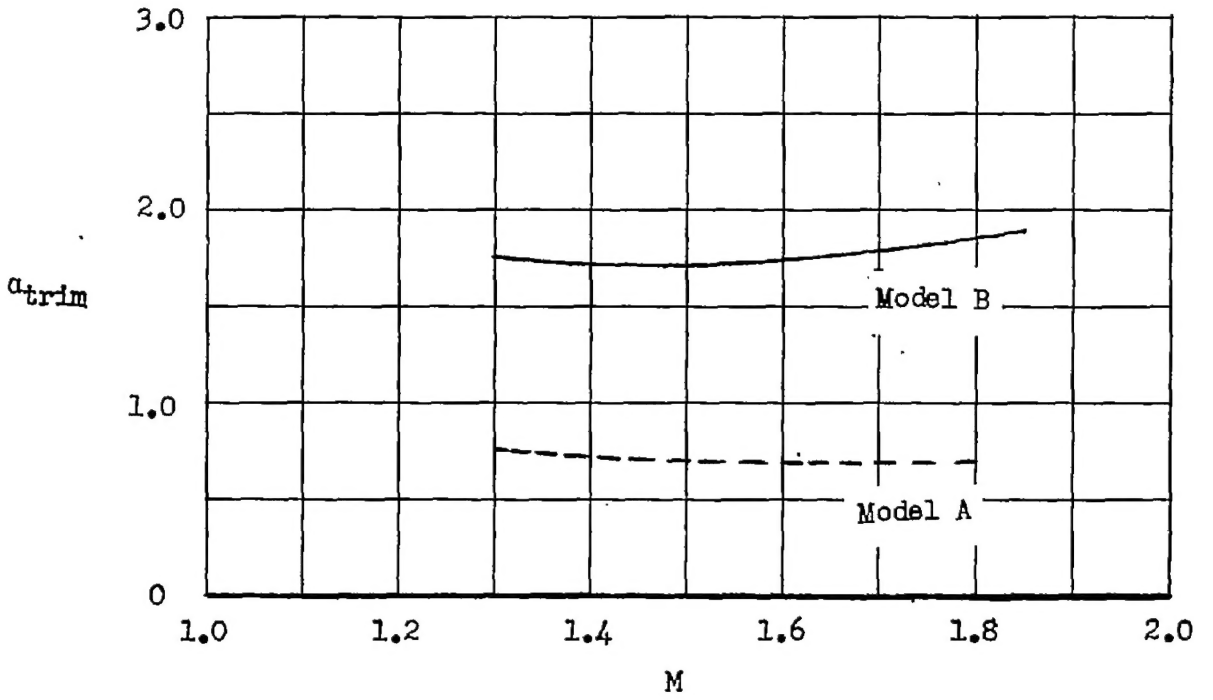

Figure 9.- Trim angle-of-attack variation with Mach number.

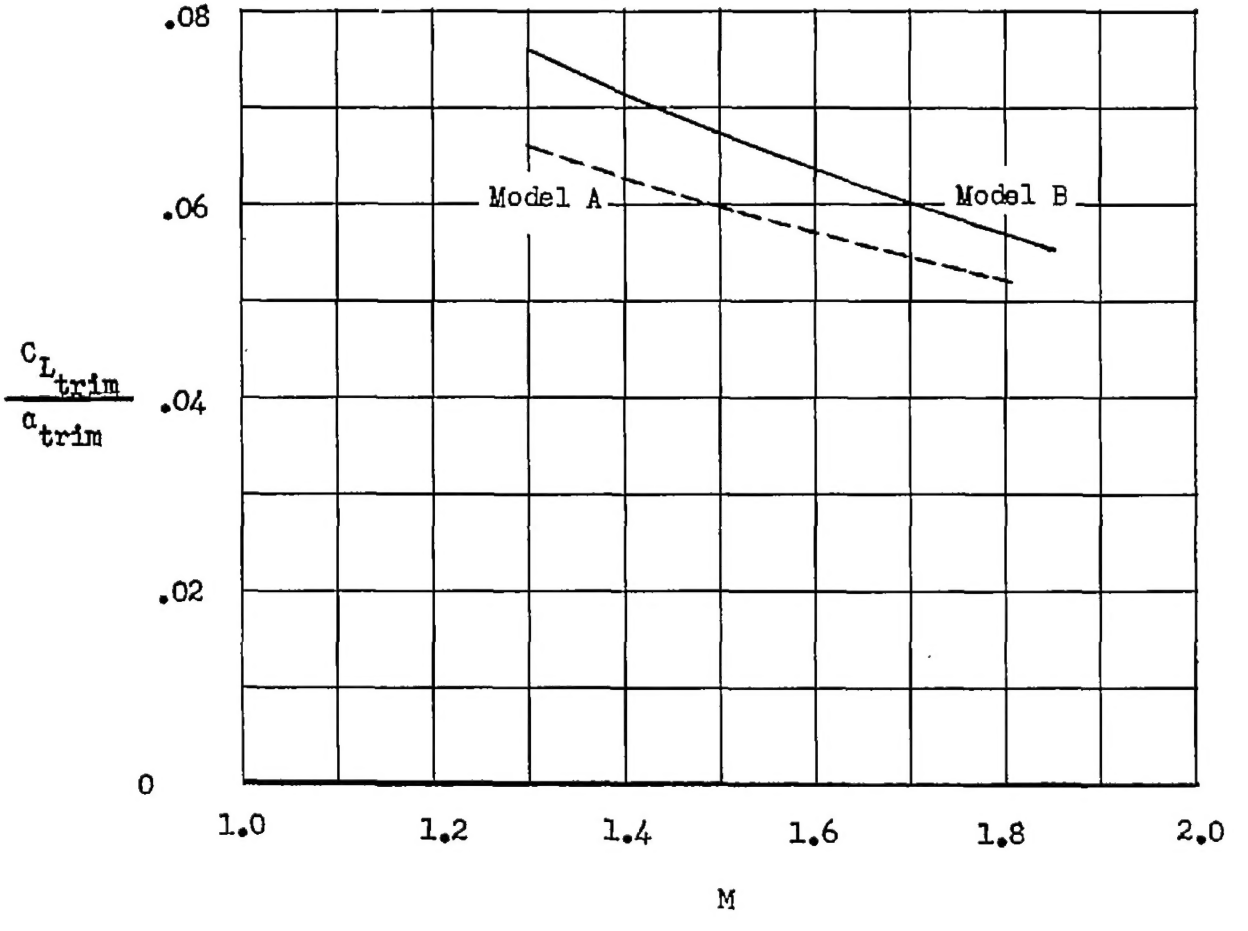

Figure 10.- Variation of approximate trim lift-curve slope with Mach number.

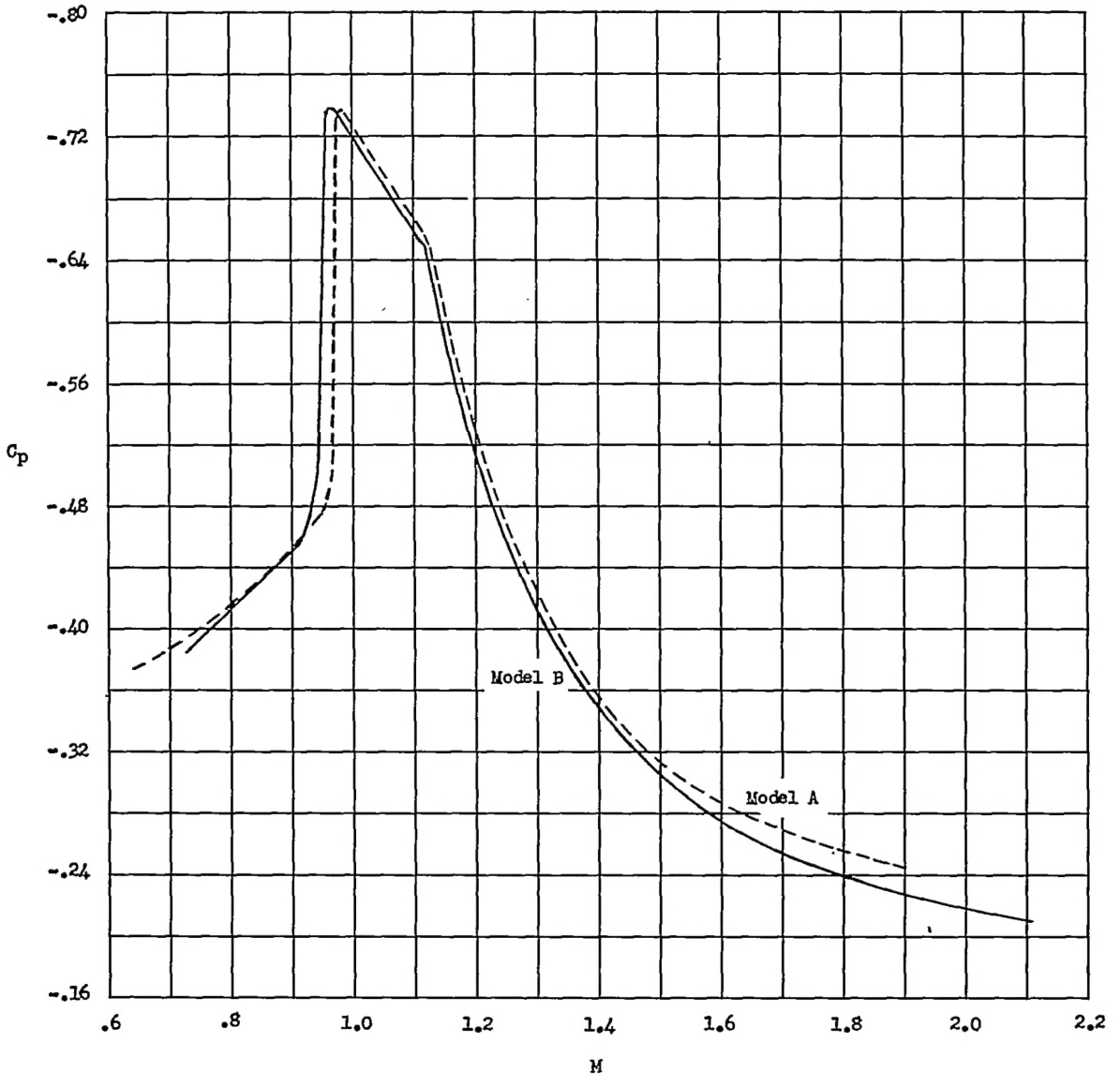

Figure 11.- Variation of nacelle annular base pressure coefficient with Mach number.

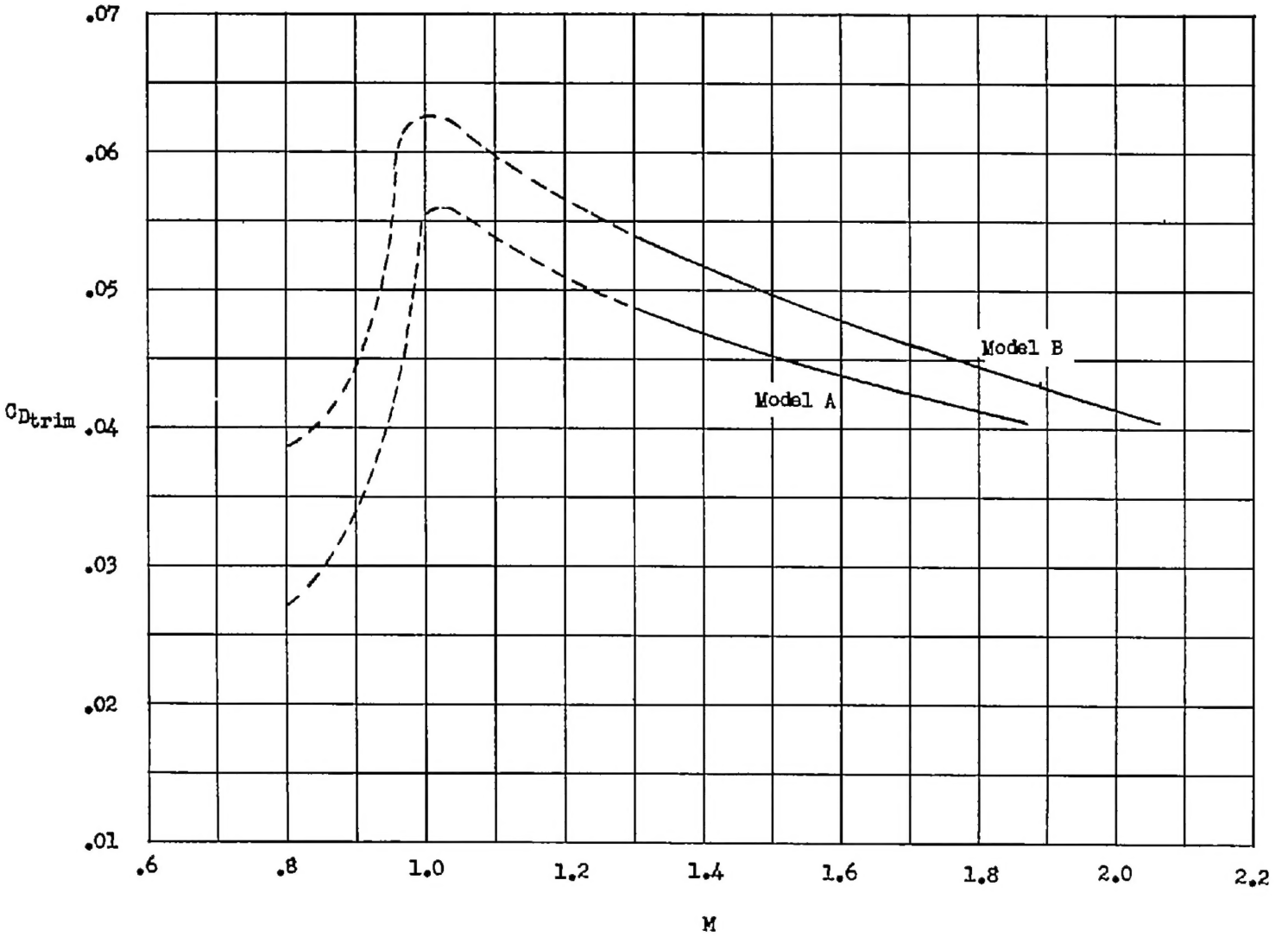

Figure 12.- Variation with Mach number of measured trim drag coefficient minus nacelle internal and base drag coefficients.